SUPPLEMENTAL DATA

125 162
ESARNPTIYPLTLPPALSSDPVIIGCLIHDYFPSGTMNVTWGKSGKDITTVNFPPALASG

185 228
GRYTMSSQLTLPAVECPEGESVKCSVQHDSNPVQELDVNCSGPTPPPPITIPSCQPSLSL

245
QRPALEDLLLGSDASITCTLNGLRNPEGAVFTWEPSTGKDAVQKKAVQNSCGCYSVSSVL

305
PGCAERWNSGASFKCTVTHPESGTLTGTIAKVTVNTFPPQVHLLPPPSEELALNELLSLT

365
CLVRAFNPKEVLVRWLHGNEELSPESYLVFEPLKEPGEGATTYLVTSVLRVSAETWKQGD

425 438 453
QYSCMVGHEALPMNFTQKTIDRLSGKPTNVSVSVIMSEGDGICY

Figure S1. *O*- and *N*-glycosylation sites in the Fc region of 6-19 IgA mAb bearing the *Igh-2*^{a} allotype. The 62 amino-acid hinge peptide yielded by treatment with trypsin and lysylendopeptidase is underlined, with the hinge region highlighted in blue. The *O*-linked glycosylation site at threonine position 228 and three *N*-linked glycosylation sites at N162, N438 and N453 are boxed.

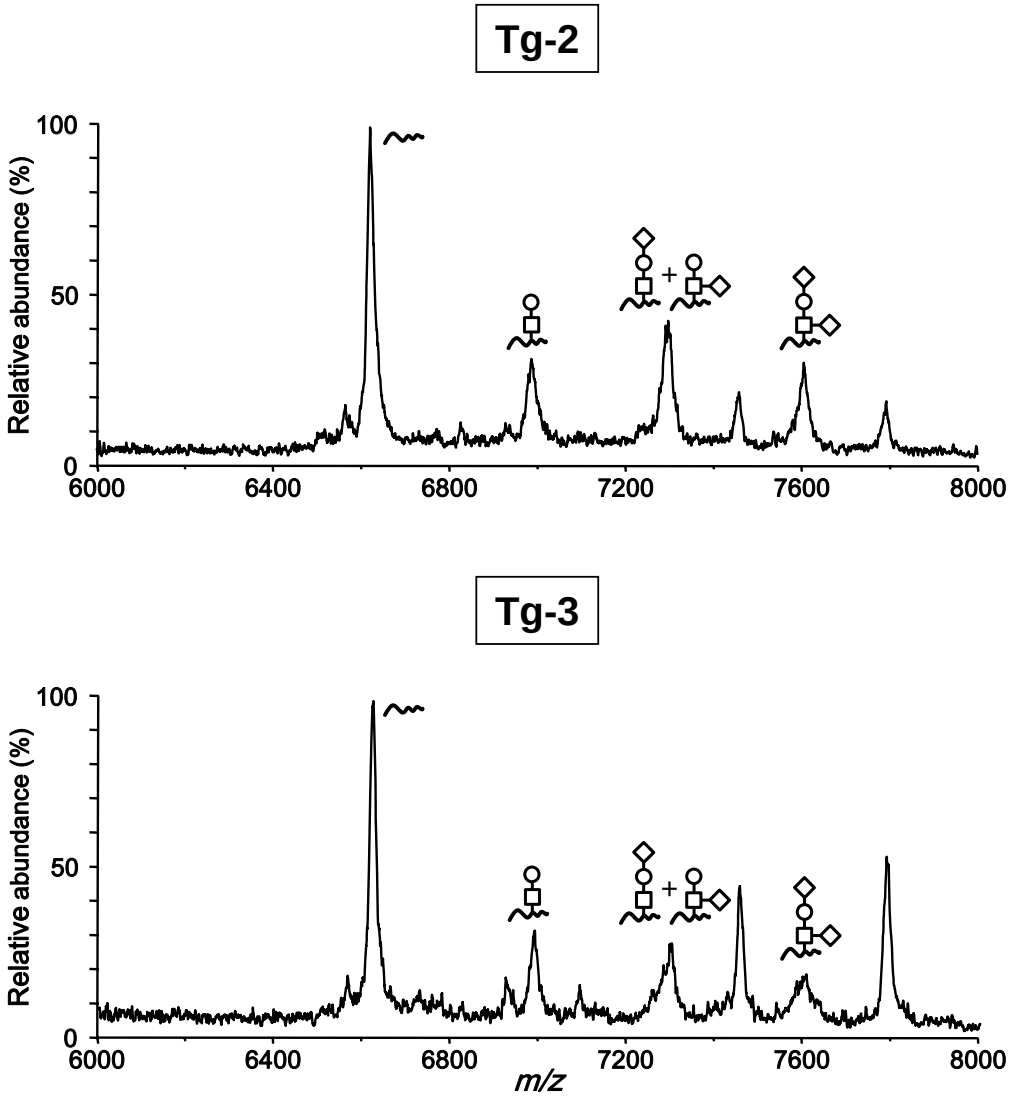

Figure S2. MALDI linear-TOF mass spectra of glycopeptides bearing *O*-glycans from the hinge region of 6-19 Tg-2 and Tg-3 IgA mAbs. The glycoforms are indicated above the corresponding glycopeptide peaks (open square: *N*-acetylgalactosamine; open circle: galactose; open diamond: *N*-glycolylneuraminic acid). Peaks without indication of glycoforms were derived from other peptides. *m*/*z*: mass-to-charge ratio.

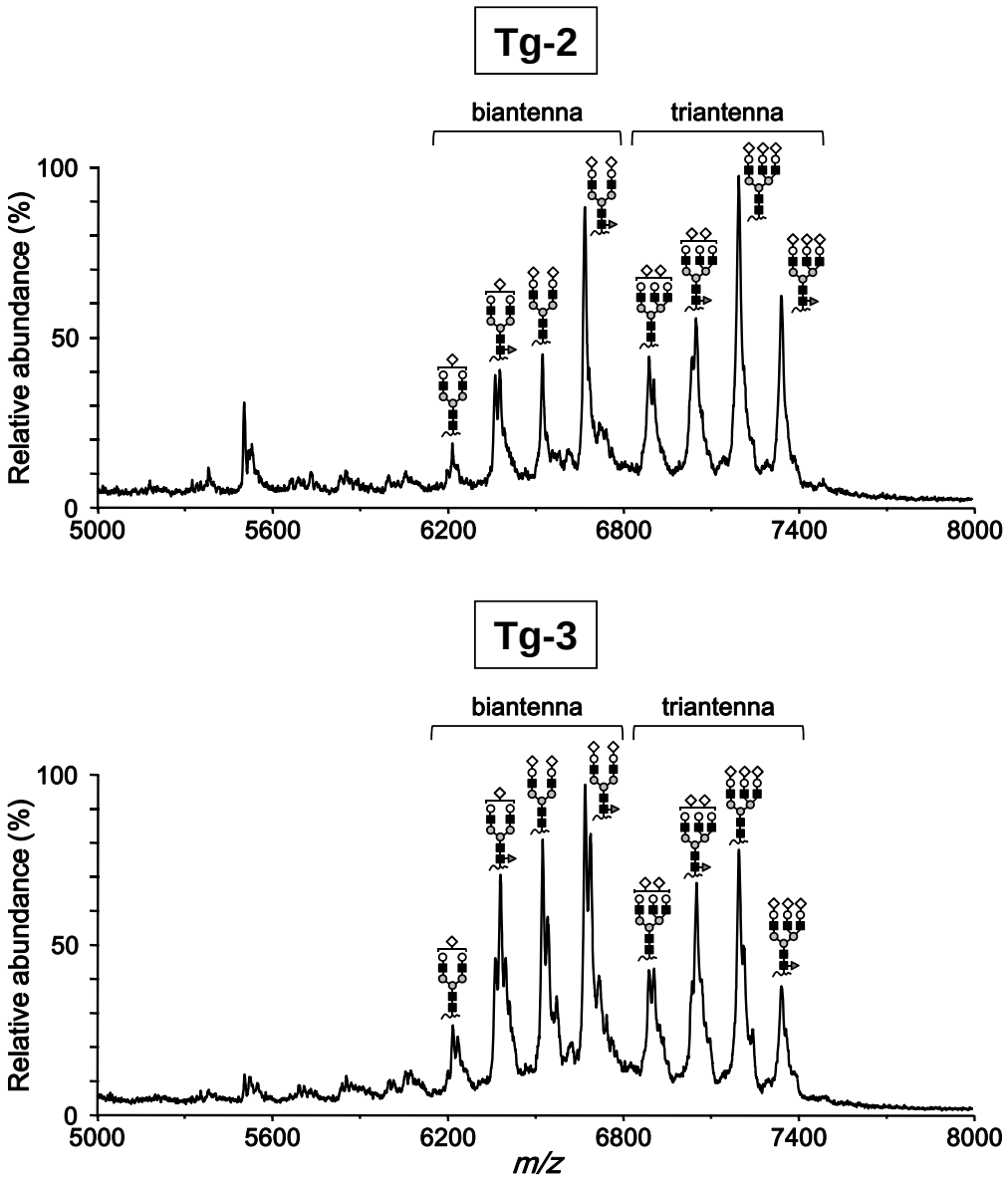

Figure S3. MALDI linear-TOF mass spectra of glycopeptides bearing *N*-glycans attached to N162 in the CH1 domain of 6-19 Tg-2 and Tg-3 IgA mAbs. The glycoforms are indicated above corresponding glycopeptide peaks (closed square: *N*-acetylglucosamine; gray circle: mannose; open circle: galactose; open diamond: *N*-glycolylneuraminic acid; dark gray triangle: fucose). Peaks without indications of glycoforms were derived from other peptides.

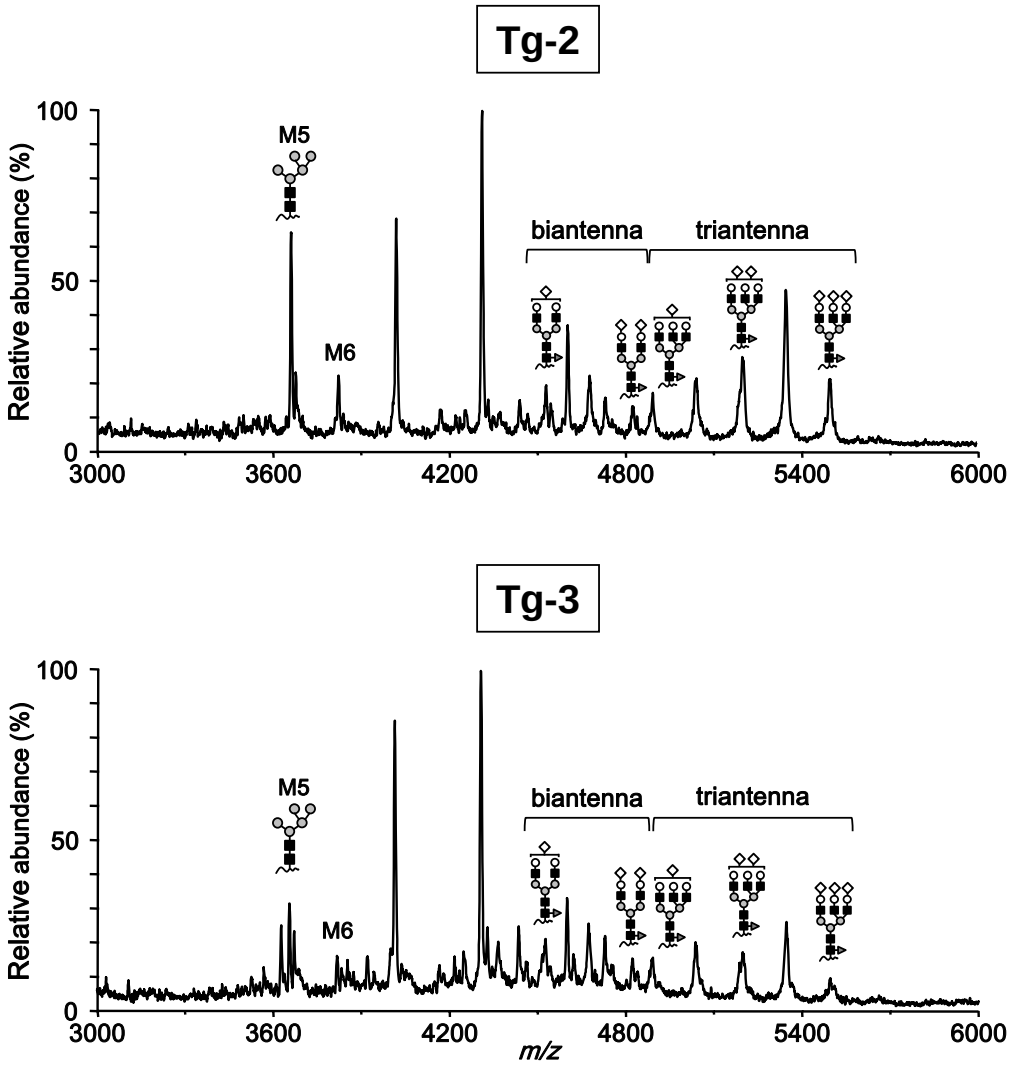

Figure S4. MALDI linear-TOF mass spectra of glycopeptides bearing *N*-glycans attached to N438 in the CH3 domain of 6-19 Tg-2 and Tg-3 IgA mAbs. The glycoforms are indicated above corresponding glycopeptide peaks. M5 and M6 indicate the high mannose-type oligosaccharides containing five and six mannose residues, respectively Peaks without indications of glycoforms were derived from other peptides.

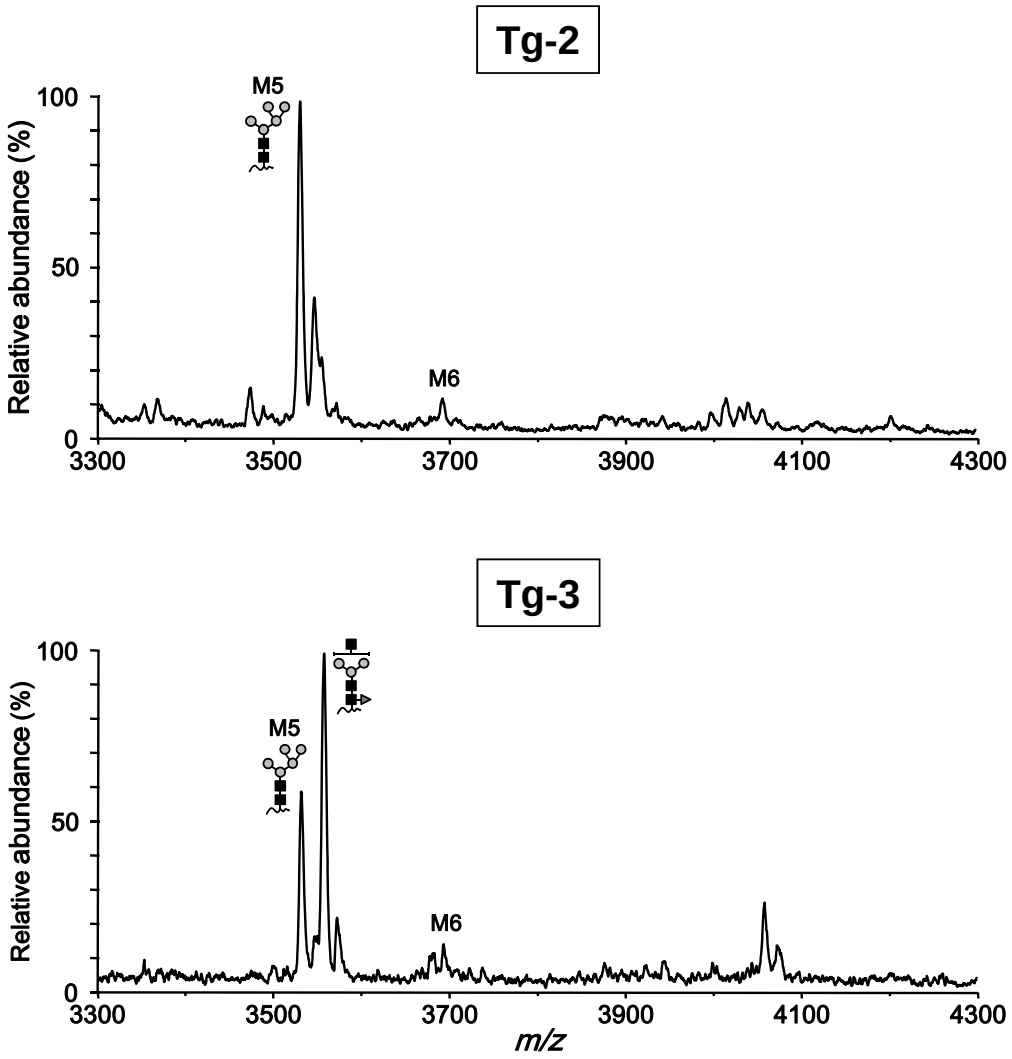

Figure S5. MALDI linear-TOF mass spectra of glycopeptides bearing *N*-glycans attached to N453 in the secretary tailpiece of 6-19 Tg-2 and Tg-3 IgA mAbs. Note the presence of high mannose-type and complex-type glycoforms in Tg-3 IgA, but the presence of only high mannose-type in Tg-2 IgA. The glycoforms are indicated above corresponding glycopeptide peaks, and peaks without indication of glycoforms were derived from other peptides.

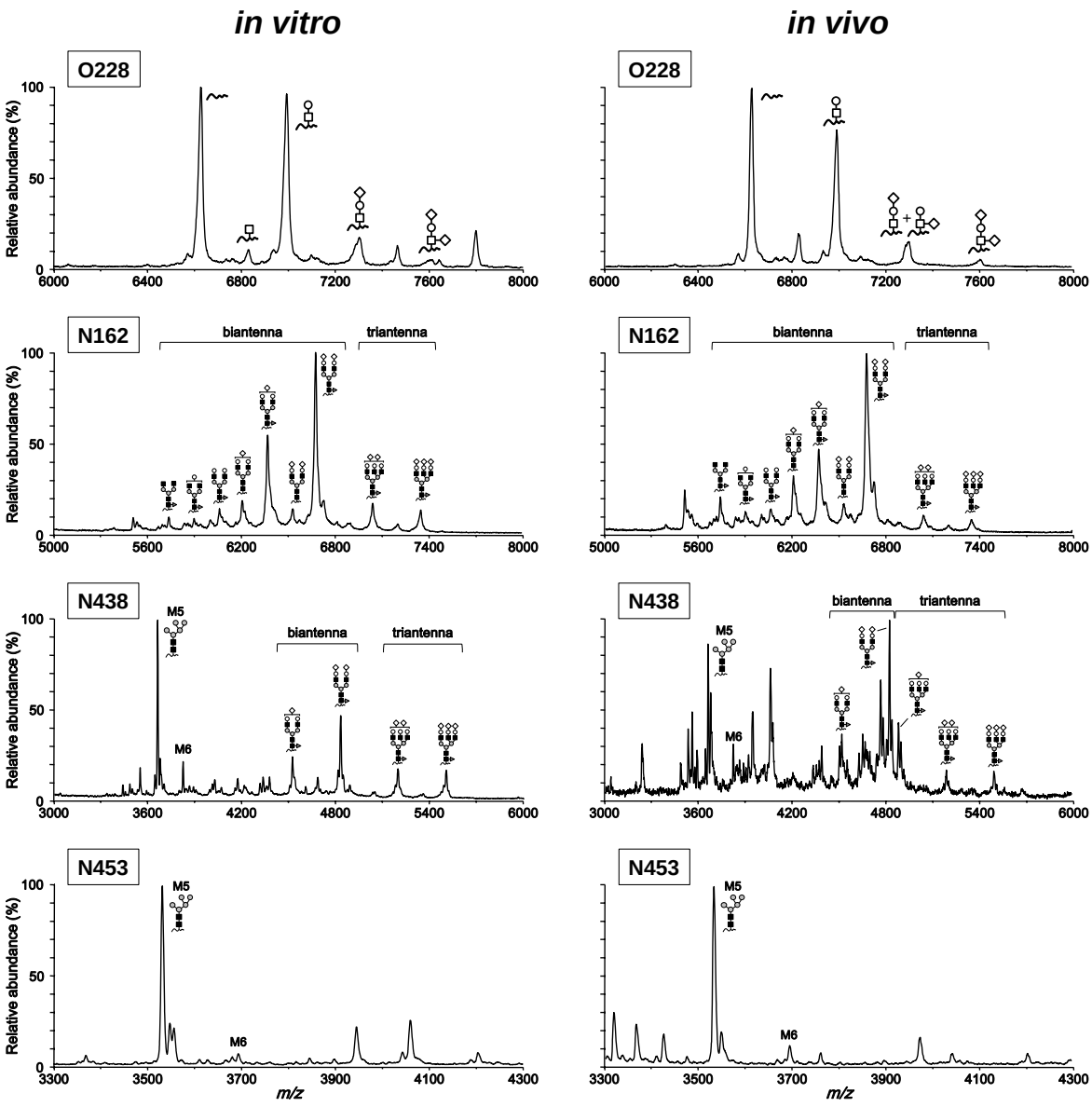

Figure S6. MALDI linear-TOF mass spectra of glycopeptides bearing *O*-glycans in the hinge region (**O228**) or *N*-glycans in the CH1 (**N162**) and CH3 (**N438**) domains and the secretary tailpiece (**N453**) of WT 6-19 IgA purified from culture supernatant (left panel) or from ascites of mice implanted with WT 6-19 IgA hybridoma (right panel). Note that the glycosylation patterns of *O*- and *N*-glycans in the *in vitro* and *in vivo* settings were comparable. The glycoforms are indicated above the corresponding glycopeptide peaks, and peaks without indication of glycoforms were derived from other peptides.

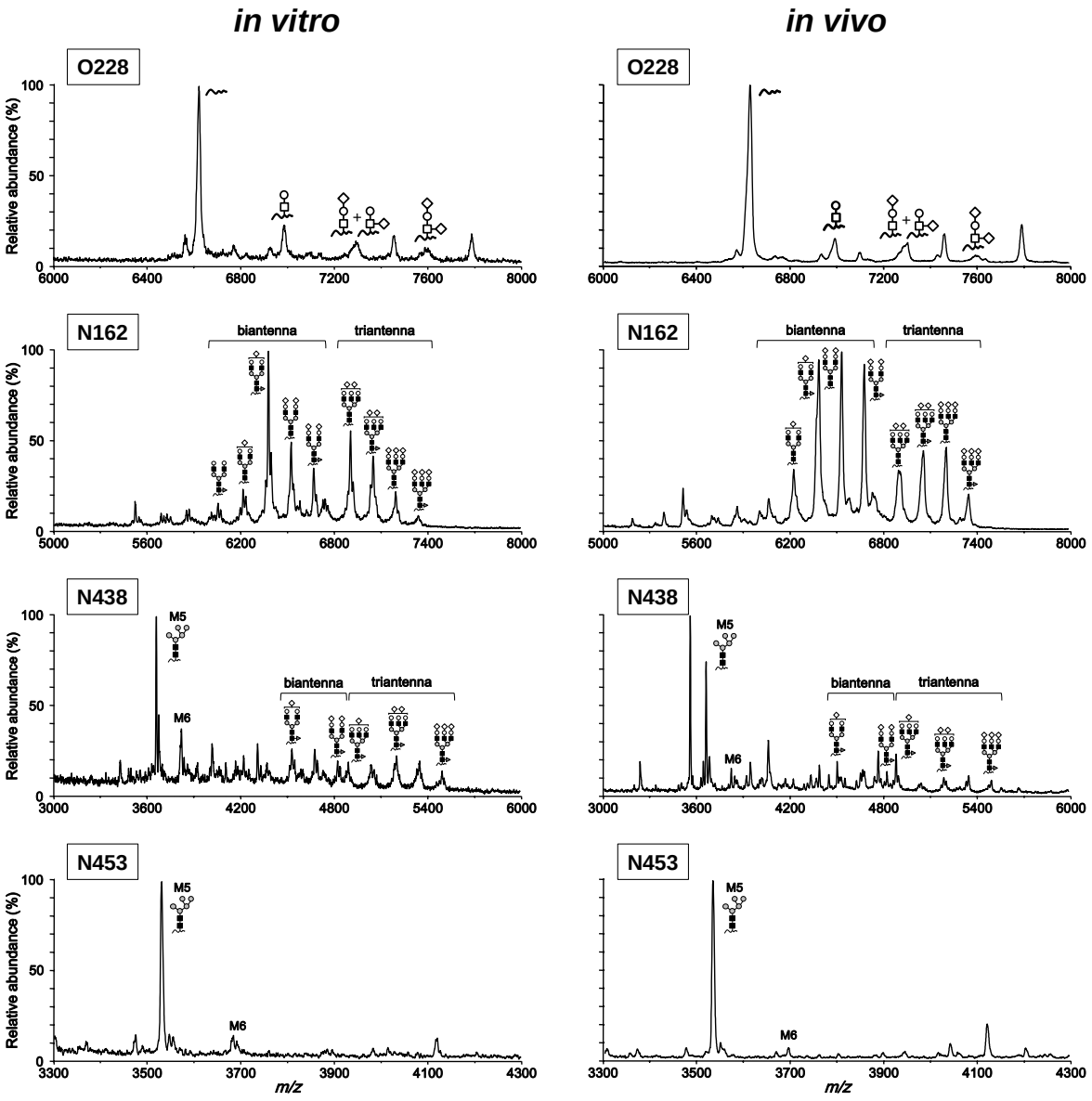

Figure S7. MALDI linear-TOF mass spectra of glycopeptides bearing *O*-glycans in the hinge region (**O228**) or *N*-glycans in the CH1 (**N162**) and CH3 (**N438**) domains and the secretary tailpiece (**N453**) of 6-19 Tg-1 IgA purified from culture supernatant (left panel) or from ascites of mice implanted with 6-19 Tg-1 IgA hybridoma (right panel). As observed with 6-19 WT IgA, the glycosylation patterns of *O*- and *N*-glycans in the *in vitro* and *in vivo* settings were comparable. Notably, this was also the case of Tg-2 and Tg-3 IgAs (data not shown). The glycoforms are indicated above the corresponding glycopeptide peaks, and peaks without indication of glycoforms were derived from other peptides.